

Science Highlights from NASA's New Horizons Mission

Harold A. Weaver, S. Alan Stern, Leslie A. Young, John R. Spencer, Catherine B. Olkin, Andrew F. Cheng, and Ralph L. McNutt Jr.

ABSTRACT

NASA's New Horizons (NH) mission was the first to explore Pluto and the Kuiper Belt in situ. Launched on January 19, 2006, the spacecraft successfully executed close flybys of Jupiter on February 28, 2007, Pluto on July 14, 2015, and the small Kuiper Belt object (KBO) Arrokoth on New Year's Day 2019. NH transformed Pluto from a barely resolved astronomical target into a geologically complex and diverse world with hints of a subsurface ocean. NH data showed Charon to be very different from Pluto, with a surface dominated by water ice but sprinkled with ammonia-bearing ices near some craters, a giant chasm nearly encircling its equator, and a reddish polar hood. Pluto's small satellites were resolved for the first time by NH, and spectra of Nix and Hydra showed deep absorption bands of water ice, strengthening the hypothesis that these small satellites formed ~4.5 billion years ago in the aftermath of the same cosmic collision that produced the Pluto–Charon binary. NH observations revealed Arrokoth to be a “contact binary” with two highly flattened lobes and an organic-rich surface showing traces of methanol ice but essentially devoid of water ice. The NH Arrokoth data provide some of the first detailed evidence for the “pebble cloud collapse” streaming instability model of planetesimal formation in the solar nebula. NH returned unique scientific results during its flyby of Jupiter; data from its plasma instruments during the mission's cruise phases are revealing new insights into the solar wind and the outer heliosphere, and NH observations of distant (i.e., non-flyby) KBOs provide data at geometries unattainable from Earth-based facilities, enabling unique results on light scattering from KBO surfaces. The NH instruments and spacecraft are still as capable as they were at launch more than 17 years ago, and they are continuing their exploration of the outer solar system and beyond during a recently approved second extended mission phase.

INTRODUCTION

The New Horizons (NH) mission was selected by NASA in November 2001 to perform the first in situ exploration of Pluto and the Kuiper Belt.¹ The Kuiper

Belt is a roughly torus-shaped region extending approximately from Neptune's orbit at a heliocentric distance of 30 au (1 au, or astronomical unit, is the average

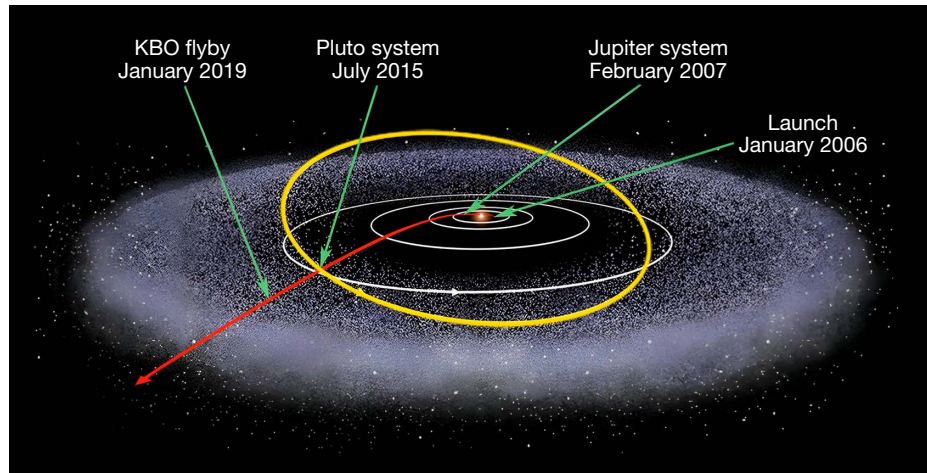


Figure 1. Artist's depiction of the NH spacecraft trajectory across the solar system covering both the prime and first extended (KEM1) mission portions. The Sun is the bright orange dot at the center. Moving outward from the Sun, the white circles show the nearly circular orbits of Jupiter, Saturn, Uranus, and Neptune. The Kuiper Belt is schematically illustrated by a roughly doughnut-shaped region filled with little white dots, which represent individual KBOs. The yellow curve is the inclined elliptical orbit of Pluto, which crosses the ecliptic plane (the plane containing the Sun and planets) at the same time the spacecraft reached Pluto in July 2015 at a heliocentric distance of 32 au. The NH journey began with the launch in January 2006, and the spacecraft received a gravity boost during the Jupiter flyby in February 2007. The close flyby of KBO Arrokoth occurred on January 1, 2019, and the spacecraft has continued to move farther from the Sun ever since.

Earth–Sun distance) to about 100 au from the Sun (Figure 1). Pluto is an iconic member of the Kuiper Belt: it was the first Kuiper Belt object (KBO) discovered (in 1930 by Clyde Tombaugh at the Lowell Observatory in Flagstaff, Arizona), is the Kuiper Belt's largest known body (thereby qualifying as a “dwarf planet”), and has an orbit that essentially extends across the entire classical Kuiper Belt (30–50 au, not including the full orbits of the so-called scattered KBOs).

The discoveries, starting in the 1990s, of hundreds of other KBOs, including several families of bodies with different orbital characteristics, motivated a revolution in the models describing how the solar system formed and evolved over time. It soon became clear that understanding the roles of Pluto and other KBOs would be key to producing a comprehensive picture of the genesis and subsequent evolution of the solar system. Thus, the scientific community urged NASA to support a mission that could explore Pluto and the KBOs at close range,² and this culminated in the selection of NH as the first of what was to become NASA's New Frontiers category of midsize planetary missions led by individual principal investigators. The NH spacecraft was launched on January 19, 2006, and successfully executed close flybys of Jupiter on February 28, 2007, Pluto on July 14, 2015 (completing the primary mission phase after the downlink of all the Pluto-system data in late 2016), and the small KBO Arrokoth (during the first extended mission phase, called Kuiper Belt Extended Mission 1, or KEM1)

on New Year's Day 2019 (January 1, 2019).

NH investigations produced new and unique scientific results during all three flybys and during the cruise phases before and after the flybys. We attempt to cover the highlights in this article, but space limitations mean that many details must be omitted, and even some major results are not included. To partially remedy these shortcomings, we point the reader to several other sources that are more comprehensive in their coverage of NH science results. The recently published book *The Pluto System after New Horizons*³ (PSANH, a volume in the University of Arizona Space Science Series; several chapters are explicitly referenced later) has 25 chapters and provides important his-

torical context as well a systematic review of the science results from NH's exploration of the outer solar system. This book should serve as the fundamental reference for Pluto system studies for at least the next decade. Three recent review articles on NH results, one from an astronomical and cosmogonical perspective,⁴ one focusing more on geology,⁵ and one on Pluto's atmosphere,⁶ can also be consulted by readers seeking more details. Another review paper lays out the objectives of NH's KEM1 phase,⁷ and a chapter in the PSANH book summarizes the results from the Arrokoth flyby.⁸

Finally, we note that the NH instruments and spacecraft are still as capable as they were at launch more than 17 years ago, and they are continuing their exploration of the outer solar system and beyond during a recently approved second extended mission phase, KEM2, which started in late 2022.

NH SCIENCE OBJECTIVES

The scientific objectives of the NH prime mission (i.e., up through the Pluto flyby) were initially defined in a NASA announcement of opportunity (AO),⁹ which itself was informed by the findings of a community-based science committee convened by NASA in the early 1990s.¹ After NH was selected, approved for flight, and launched, detailed science requirements for the mission were defined in NASA's Program-Level Requirements Appendix (PLRA). The PLRA essentially serves as a

contract between NASA and the NH project and is used to define mission success criteria.

The high-level science objectives of the NH prime mission are succinctly summarized below. Group 1 objectives are the “must-have” highest-priority objectives required to achieve “minimum mission success”; Group 2 objectives are “highly desirable”; and Group 3 objectives are “desirable, if possible.” Each high-level objective is associated with detailed science requirements in the AO and the PLRA, and these detailed requirements drove the mission’s design and the instrument specifications (as discussed in the other articles in this issue). NH achieved full mission success for the prime mission by achieving all the science objectives listed below, in addition to conducting a successful Jupiter science flyby (which had no specific science objectives) and a successful KBO flyby (with science objectives similar to many of those listed below but specified for Arrokoth in a separate KEM1 PLRA). Discussion of how each objective was met is outside the scope of this article; rather, the intent is to summarize some of the key science results from the mission.

Group 1 Objectives

- Characterize the global geology and morphology of Pluto and Charon.
- Map the surface composition of Pluto and Charon.
- Characterize the neutral atmosphere of Pluto and its escape rate.

Group 2 Objectives

- Characterize the time variability of Pluto’s surface and atmosphere.
- Image Pluto and Charon in stereo.
- Map the terminators of Pluto and Charon with high resolution.
- Map the composition of selected areas of Pluto and Charon at high resolution.
- Characterize Pluto’s ionosphere and solar wind interaction.
- Search for neutral species including H, H₂, HCN, and C_xH_y, and other hydrocarbons and nitriles in Pluto’s upper atmosphere.
- Search for an atmosphere around Charon.
- Determine bolometric Bond albedos for Pluto and Charon.
- Map the surface temperatures of Pluto and Charon.
- Characterize the global geology and morphology of Nix and Hydra.
- Map the surface composition of Nix and Hydra.

Group 3 Objectives

- Characterize the energetic particle environment of Pluto and Charon.
- Refine bulk parameters (radii, masses, densities) and orbits of Pluto and Charon.
- Search for additional satellites and rings.

SCIENCE PLANNING

The NH science team developed rigorous processes to optimize the mission’s science return. The team’s expertise focused mainly on Pluto, the Kuiper Belt, and the small bodies of the solar system, so the broader planetary science community supplemented the team’s capabilities for the Jupiter flyby. Several well-known experts on the Jovian system came onboard temporarily (becoming part of the Jupiter encounter science team, led by NH co-investigators) to help design and plan an ambitious set of observations starting in January 2007 and continuing through the end of March. In fact, the number of observations planned for the Jupiter flyby, and the planned data volume, significantly exceeded the original strawman plan for the Pluto flyby. The Jupiter flyby essentially amounted to a stress test for the NH team, and the team passed with flying colors, as documented by the exciting scientific results discussed later.

Employing lessons learned from the Jupiter flyby, in late 2007 the NH science team embarked on an even more ambitious project to plan the details of the Pluto flyby. For the primary mission phase, the NH science team was organized around four themes: (1) geology, geophysics, and imaging; (2) surface composition; (3) atmospheres; and (4) particles and plasma. For KEM1, the latter two teams were condensed into the particles and atmospheres team.

The Pluto encounter planning (PEP) team formed in 2007 (during the primary mission phase) to synthesize the objectives of each theme team and to design an observation plan for the Pluto flyby that would optimize the scientific return while still fulfilling the mission’s PLRA requirements. The PEP team formulated measurement techniques for each of NH’s objectives, including the primary measurements (those with the highest performance for a particular objective), backup measurements (typically with slightly degraded performance) for redundancy, and alternate measurements (usually implemented only for the Group 1 objectives) in case the instrument(s) used for the primary measurements were not available. The PEP team planned an extensive campaign to observe the Pluto system; it began in January 2015 with the first approach-phase observations and ended about a year later with the final departure-phase observations.

The measurement techniques typically contained one-page descriptions, maintained on a team wiki, describing the motivation for the observations and the measurements required to achieve the science objectives. Various software tools were developed to assist team members in designing the timing and the instrument details needed to achieve the objectives. By early 2009, the PEP team had designed a consensus timeline covering the 9 days around Pluto closest approach (CA), the so-called platinum load (CA–7 days to CA+2 days, inclusive), when essentially all the NH science objectives would be addressed, and this load was put under configuration control in 2010. Most of the platinum load was successfully tested during an in-flight rehearsal in July 2013, and the full load ran flawlessly during the actual Pluto flyby in July 2015. The scientific highlights from the Pluto flyby are discussed below.

The PEP effort ended after the Pluto flyby, but most of its functionality was resurrected in 2016 to design and implement the KEM1 observations, most importantly the flyby observations of Arrokoth. Although the time between the planning and the execution of the Arrokoth flyby was much shorter than that for the Pluto flyby, the lessons learned during the PEP process facilitated the relatively rapid planning for the Arrokoth campaign. As for Pluto, the NH team developed a 9-day platinum load for the Arrokoth flyby that contained the

most important science observations. Although there was no in-flight rehearsal of this load, extensive ground testing and the experience gained from the Pluto flyby enabled an essentially perfect execution of the load during the last week of 2018 and the first few days of 2019. The scientific highlights from the Arrokoth flyby are discussed below.

Although NH made its most important observations during the three flybys (Jupiter, Pluto, and Arrokoth), it also conducted unique and revolutionary science during the cruise phases that were not associated with any particular flyby. The planning of these cruise observations followed the same rigorous design, development, and review process that governed the entire mission. Some of the cruise mission science highlights are discussed below.

SCIENCE HIGHLIGHTS

Pluto Flyby Results

Pluto

Data from NH revealed Pluto's surface to be amazingly diverse with a Texas-size nitrogen ice sheet (Sputnik Planitia, or SP; Figure 2) that drives its atmosphere, water-ice mountains as high as the Rockies in the United States, a belt of organic-rich material around its equator, and hints of a subsurface ocean.

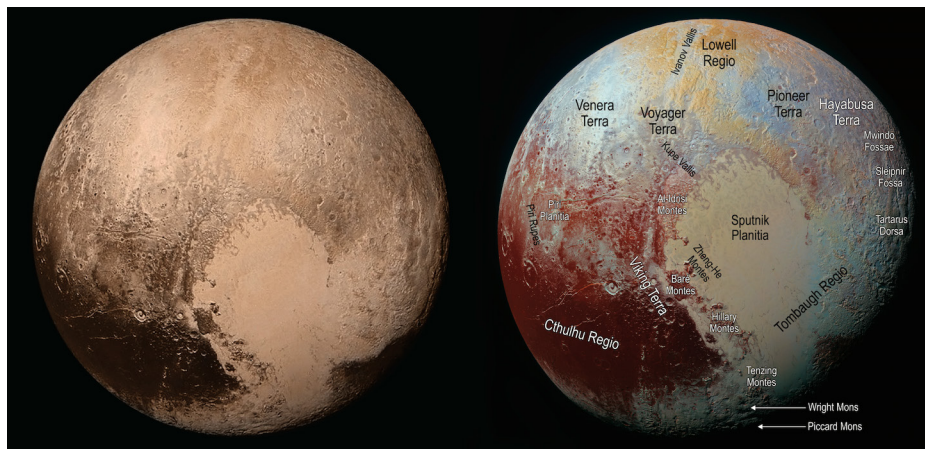


Figure 2. Two Pluto composite images. These images were produced using the final global view of Pluto from the Long Range Reconnaissance Imager (LORRI) panchromatic imager and colored using data from the Ralph Multispectral Visible Imaging Camera (MVIC) camera. The colors in the left image are rendered to show approximately the color that the human eye would see (i.e., “natural color”). The colors in the right image (adapted from Stern et al.⁴) are stretched to emphasize compositional differences across Pluto’s surface, and various regions are labeled. The left side of the heart-shaped region is a giant (~1,300 by ~1,000 km) nitrogen ice glacier named Sputnik Planitia (SP), which is brighter than most of Pluto’s surface. SP is the youngest area on Pluto, with evidence of geological activity even to the present day. The dark region near the bottom of Pluto’s globe (Cthulhu Macula, or CM) and to the left of SP is about 10 times fainter than SP, is likely composed of reddish organics, and is heavily cratered, indicating its ancient age dating back ~4 billion years. See the text for further discussion of Pluto’s extraordinary geological and compositional diversity. Pluto north is straight up and east is to the right.

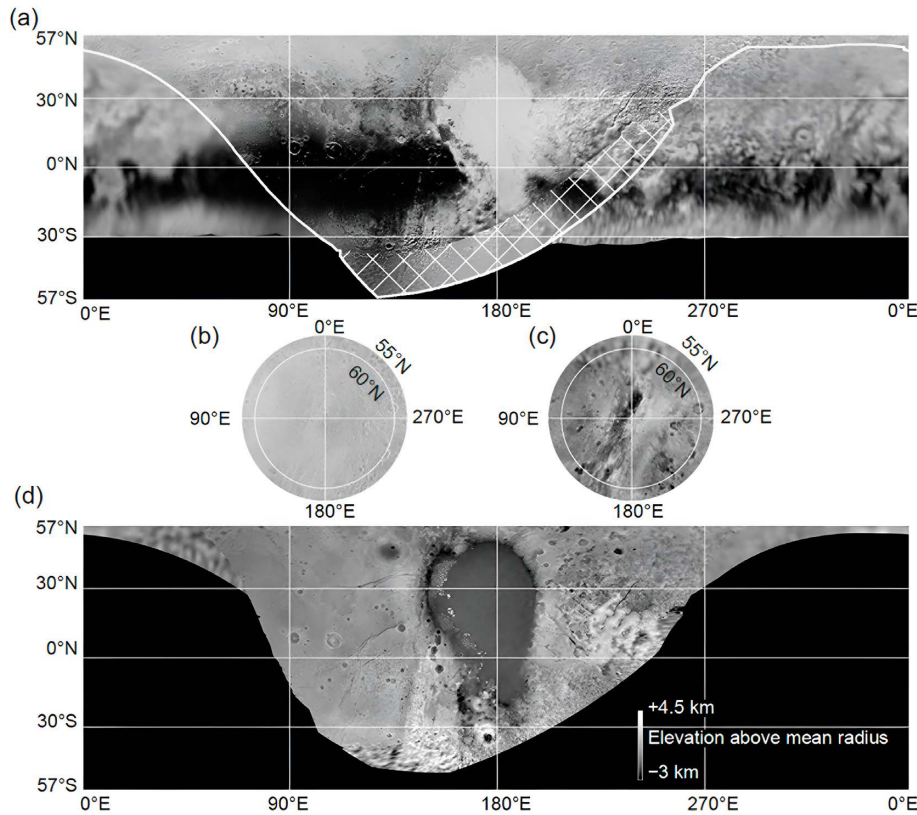


Figure 3. Pluto global map. (a and b) This map was assembled from the highest-resolution NH imaging available at various locations, shown in simple cylindrical projection between 57°N and 57°S and in polar projection north of 55°N. Black areas were not imaged by NH. The portion of Pluto imaged near the time of CA (the “nearside”) is above the white line, while the region below the white line was imaged earlier during the approach at lower resolution (the “farside”). The cross-hatched zone was illuminated by scattered sunlight from Pluto’s atmospheric haze. (c and d) Stereo digital elevation model (DEM) of Pluto’s nearside hemisphere, projected in the same manner as the mosaic. Black areas were not imaged or do not have resolvable stereogrammetric data. (Adapted from White et al.¹⁰)

Although previous Earth-based observations showed that Pluto’s surface was highly variegated (i.e., colorful) with widely varying surface reflectances (i.e., with both bright and dark regions), only the high spatial resolution provided by NH could reveal the true nature of Pluto’s surface complexity. A map using the highest-resolution NH imaging of Pluto, which covers ~78% of Pluto’s surface at different resolutions (~50% imaged at resolutions from 76 to 850 km/pixel and ~25% imaged from 2.2 to 32 km/pixel), is shown in Figure 3. Pluto’s near-side surface (i.e., the side visible to NH during CA) can be divided into six geological domains: the Sputnik, Wright, Tartarus, Hayabusa, Venera, and Burney groups (Figure 4). Some highlights of these regions are discussed below.

SP has the youngest surface on Pluto, as evidenced by the fact that no craters could be identified in its ice sheet

even in the highest-resolution LORRI images (76 m/pixel). Further evidence of this region’s youth are images showing what appears to be flow of the ice sheet around barriers (Figure 5, especially e and f). The caption to Figure 5 provides more details on SP’s geology. Figure 6 shows one of the mountain ranges (Al-Idrisi-Montes) along the northwest periphery of SP. These mountains, and some others around the edge of SP, are most likely fragments of preexisting water-ice crust that were detached from the surrounding uplands and then transported to their current locations and orientations within the flow of denser nitrogen ice.

The Wright region has intriguing surface features that seem to indicate extrusion of material from the interior, potential examples of cryovolcanism (Figure 7). Hayabusa has multiple networks of dendritic valleys,

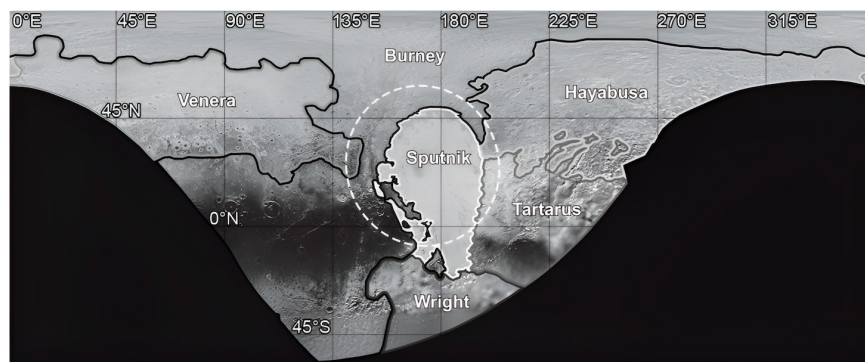


Figure 4. Mapping of the approximate boundaries of the six geological groups identified in Pluto’s nearside hemisphere (i.e., the portion of Pluto covered by imaging between 76 and 850 m/pixel). The white dashed line indicates the approximate original rim of the SP basin, assuming it was produced by an impact. The dark region near the equator is CM, which lies near the southern end of the Burney region. (Adapted from White et al.¹⁰)

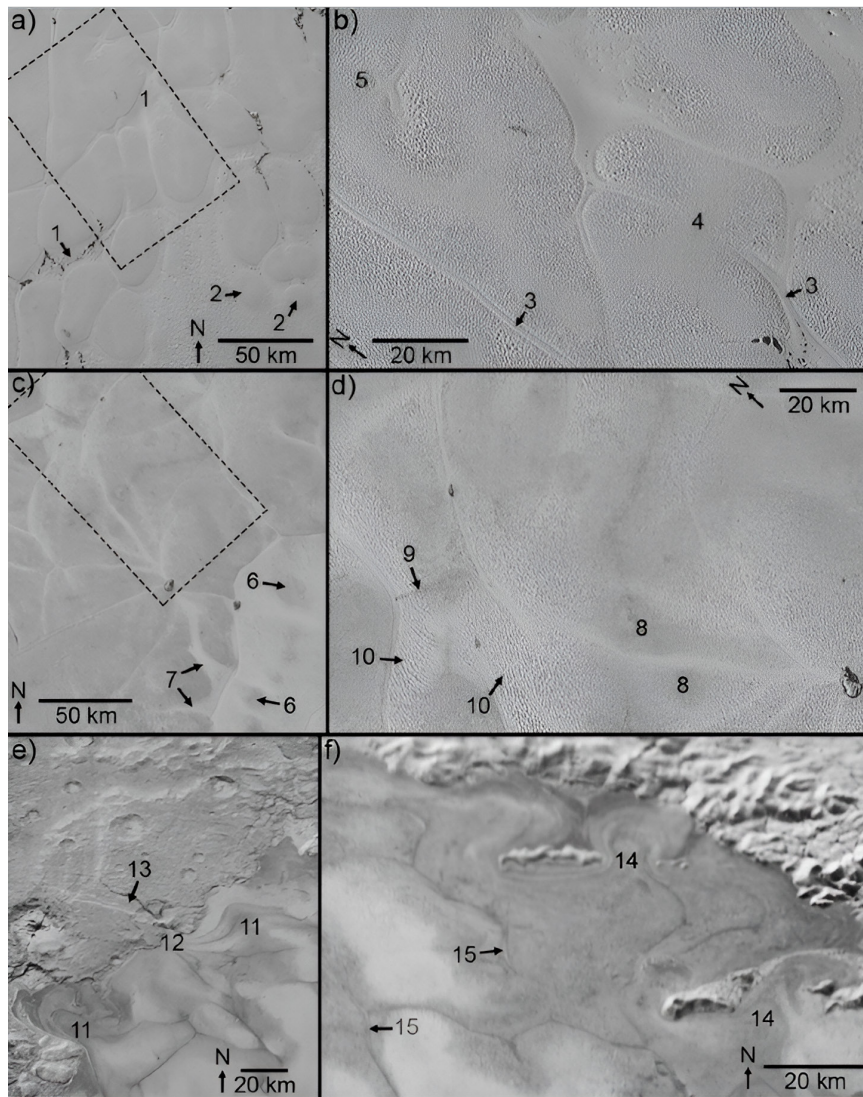


Figure 5. The amazing geological diversity in and around SP. (a) Bright cellular plains. Illumination is from the top. The dashed box indicates the boundary of the area shown in (b). 1, Interstitial expanses of noncellular plains. 2, Isolated cells at the southeast margin of the cellular plains. (b) Detail of bright cellular plains. Illumination is from the left. 3, Low, medial ridges within troughs separating the cells. 4, Smooth-textured zone cutting across a boundary between cells. 5, X-shaped junction of four troughs. (c) Contact between the dark (top left) and bright (bottom right) cellular plains. Illumination is from the top left. The dashed box indicates the boundary of the area shown in (d). 6, Enclaves of dark plains surrounded by bright plains. 7, Filaments of bright plains extending into the dark plains. (d) Detail of dark cellular plains. Illumination is from the left. 8, Smooth-textured zones extending to the cell boundaries. 9, Dark streak emanating from a cell boundary. 10, Linear texture in pitted plains. (e and f) Dark, trough-bounding plains in the northwest and northeast of SP, respectively. Illumination is from the top left. 11, Lobate flow patterns. 12, Convergence of flow bands toward the edge of SP. 13, Uplands graben intersecting SP. 14, Lobate flow patterns between nunataks. 15, Bright central lineations within dark cell boundaries. (Adapted from White et al.¹⁰)

large flat-floored pits, and pit clusters (Figure 8, a and b). Tartarus has the best examples of bladed terrain (Figure 8c), long regular ridges with methane-ice tipped peaks. These blades are likely sculpted by the direction of the solar illumination, perhaps forming giant versions of the water-ice penitentes seen in the low-latitude arctic regions of Earth.

One of the most striking features on Pluto are the dark bands encircling most of its equatorial region. The largest such band, CM, has some of the darkest and oldest terrain (Figure 9) on Pluto and comprises much of the nonpolar areas of the Burney geological domain. CM is littered with ancient craters likely dating back to the time of Pluto's formation ~4.5 billion years ago. CM is very red at optical wavelengths and is also about eight times darker than the brightest regions of SP. A plausible hypothesis is that CM is composed of organic material, produced by the rainout of aerosols from Pluto's atmosphere, by radiation (solar and interplanetary ultraviolet light, solar wind, and cosmic rays) processing of simple

hydrocarbon ices originally coating the surface, or by a combination of both processes.

How can such a small planet located so far from the Sun show this much geological diversity? The presence of highly volatile surface ices (N_2 , CH_4 , and CO) that are mobile even at Pluto's globally averaged surface temperature (~40 K) certainly helps to explain why Pluto is active geologically. In addition, a highly eccentric and tilted orbit around the Sun, and the large obliquity (~110°) of Pluto's rotational axis, produces multiple climate zones that vary over astronomical timescales (i.e., millions of years). Different latitudes on Pluto experience extremely different heating and cooling episodes over time, which certainly influences the surface morphology.

One of NH's most important scientific objectives was to map Pluto's surface composition and correlate it with geological features. This task was performed using the Linear Etalon Imaging Spectral Array (LEISA), the component of the Ralph instrument that obtained infrared spectral images of Pluto's encounter hemisphere.

Figure 6. Examples of giant water-ice mountains on Pluto. (a) Image of the mountain range of Al-Idrisi-Montes, with peaks up to ~ 7.4 km (~ 4.6 miles) high, and adjacent uplands along the northwest periphery of SP. The corresponding DEM is shown in (b). Illumination is from the right. The box in (a) indicates the boundaries of the 76-m/pixel imaging in the inset at bottom left. 1 and 2, Agglomerations of smaller and larger mountains, respectively. 3, Dark lineation crossing the face of a tilted block, which may represent layering of original crustal material that is now exposed. 4, Tilted crustal blocks separated from the uplands by broad troughs (5). (Adapted from White et al.¹⁰) (c) Color image of the southern portion of the Al-Idrisi-Montes with arrows showing two adjacent blocks with red layers visible on both vertical faces. The blocks labeled D,E,F in panel (c) correspond to the similarly labeled blocks in panel (a), but they are at different orientations. (Adapted from Olkin et al.¹¹)

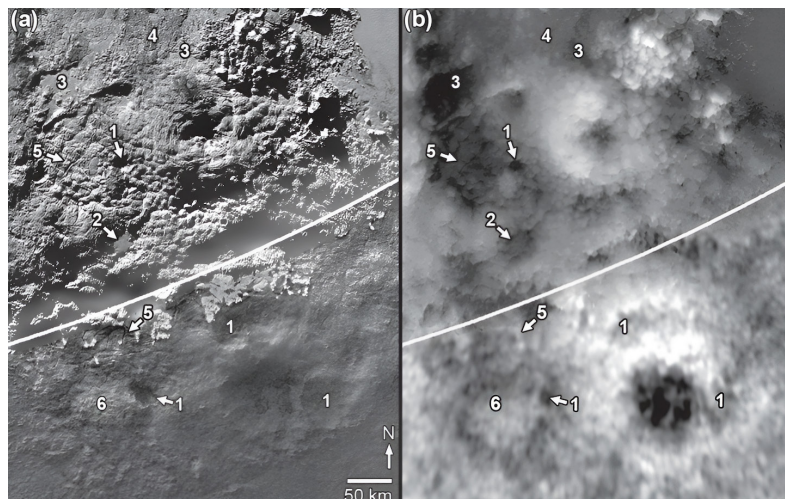
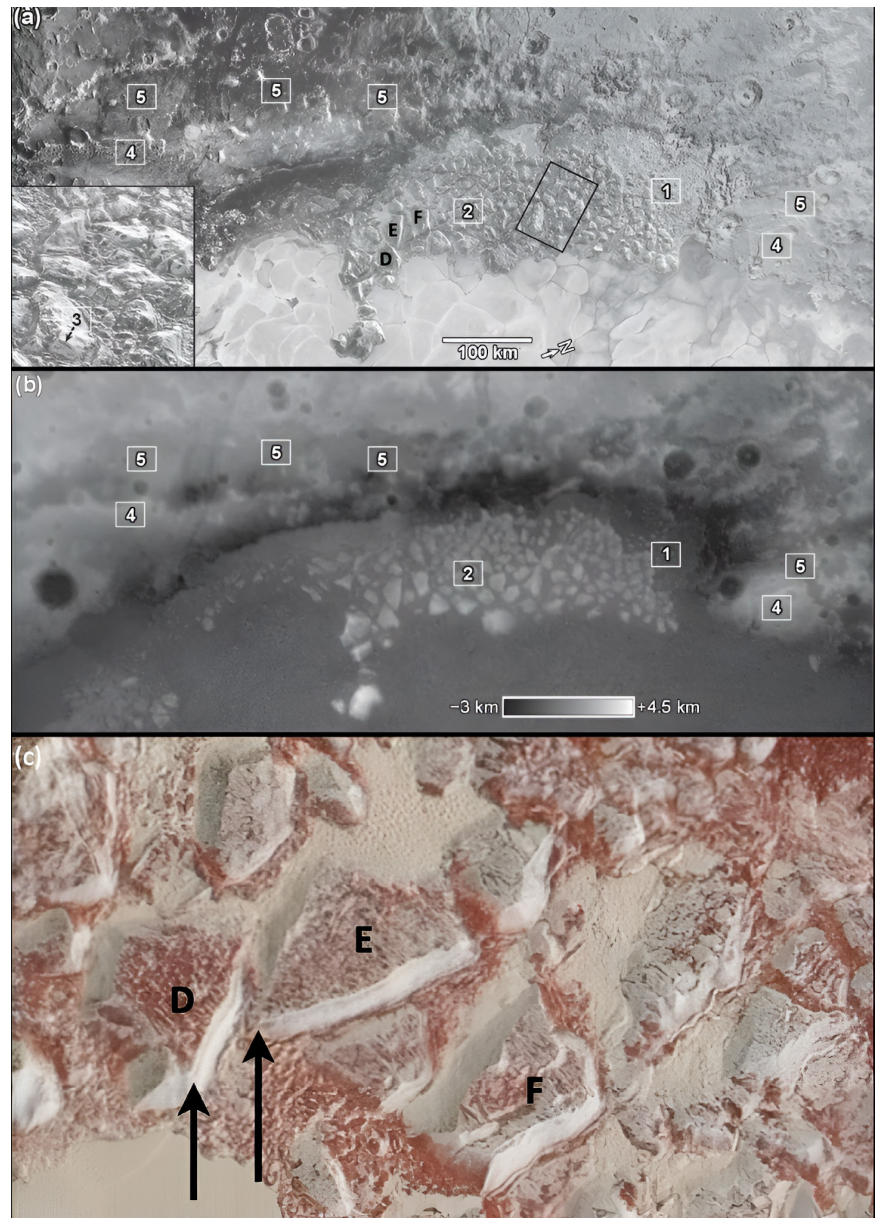


Figure 7. Two potential cryovolcanic regions within the Wright geological group. (a) Image of Wright Mons (near the upper middle) and Piccard Mons (near the lower right) and surrounding terrain. The white line marks the northern boundary of the haze-lit zone. Illumination is from the top left. 1, Rimless, dark-floored depressions (cavi). 2, Ponded nitrogen ice deposit on the floor of a cavus. 3, Nitrogen ice deposits ponded in depressions. 4, The rough blocky plain of Hyecho Palus. 5, Localized fracture networks. 6, Rough-textured dome surrounded by a trough. (b) DEM derived from the image in (a). The gray scale for the DEM ranges from -3 km (black) to $+4.5$ km (white); material is possibly erupting from below at the deepest points, which are surrounded by relatively high mounds. (Adapted from White et al.¹⁰)

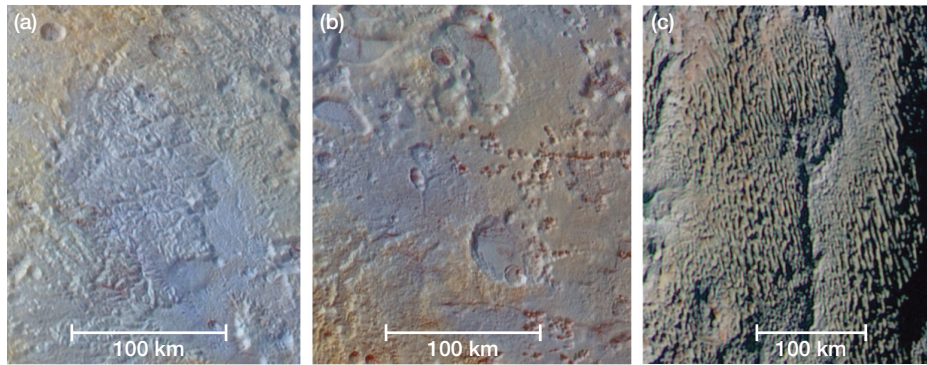


Figure 8. Three of Pluto’s distinctive geomorphologies. (a) Dendritic valley networks in Pioneer Terra, which is in the Hayabusa geological domain. (b) Irregularly shaped, flat-floored pits (upper left) and pit clusters (lower right), also in Pioneer Terra. (c) Bladed terrain in the Tartarus region. (Adapted from Stern et al.⁴)

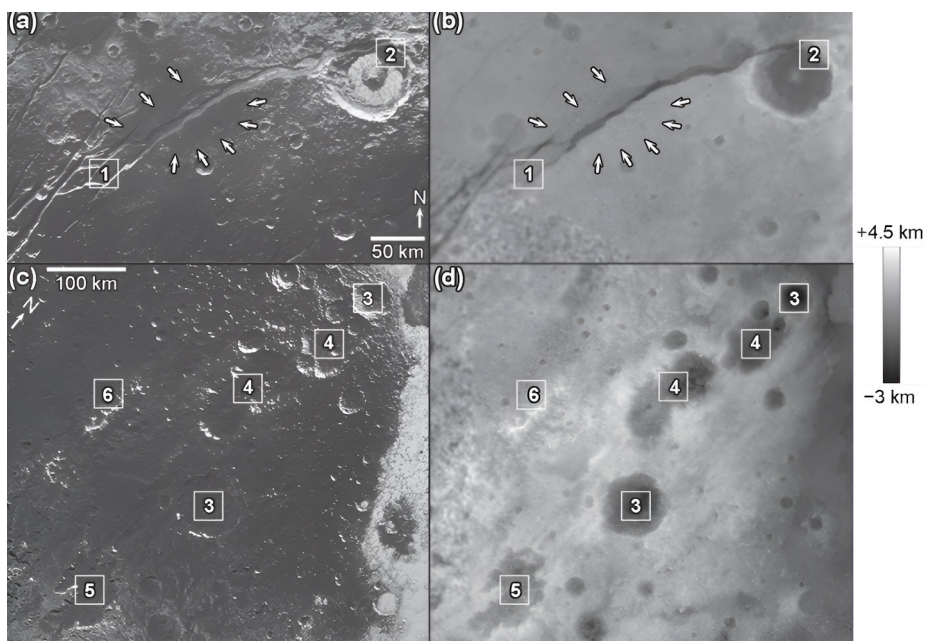


Figure 9. Two terrains in CM, which is in the Burney geological domain. Images are shown at the left, and the corresponding DEMs are to the right. (a and b) Smooth, cratered plains in the vicinity of Virgil Fossae, a large tectonic feature. The white arrows point to relatively smooth mantled terrain containing ammoniated water ice, which may have been extruded from the interior <1 billion years ago. Illumination is from the top. 1, Fractures of Hermod and Virgil Fossae crosscutting each other. 2, Virgil Fossae crosscutting Elliot crater. (c and d) Cratered and tectonized terrain in eastern CM. Illumination is from the top right. 3, Large and deep craters. 4, Large, deep, flat-floored depressions with ovoid planforms. 5, Irregular, ameboid, flat-floored depression. 6, Pigafetta Montes with bright summit regions. (Adapted from White et al.¹⁰)

Its spatial resolutions ranged from 2.8 to 7 km/pixel and with spectral resolving powers of 250 for the wavelength range 1.25–2.5 μm and 560 for the spectral range 2.1–2.25 μm . Pluto’s near-infrared spectrum is dominated by strong methane-ice absorption bands (Figure 10; all the deep bands in the spectral plots are due to methane), but LEISA has enough resolving power to detect absorptions by nitrogen, carbon monoxide, and water ice too.

By comparing detailed radiative transfer spectral models to the highest-spatial-resolution LEISA spectral images of Pluto, compositional maps of Pluto’s encounter hemisphere were constructed with an effective resolution of ~ 12 km/pixel. Figure 10 shows multiple compositional maps that are used to constrain the relative amounts of methane and nitrogen across Pluto’s surface, as well as the grain sizes needed to match the observed spectra.

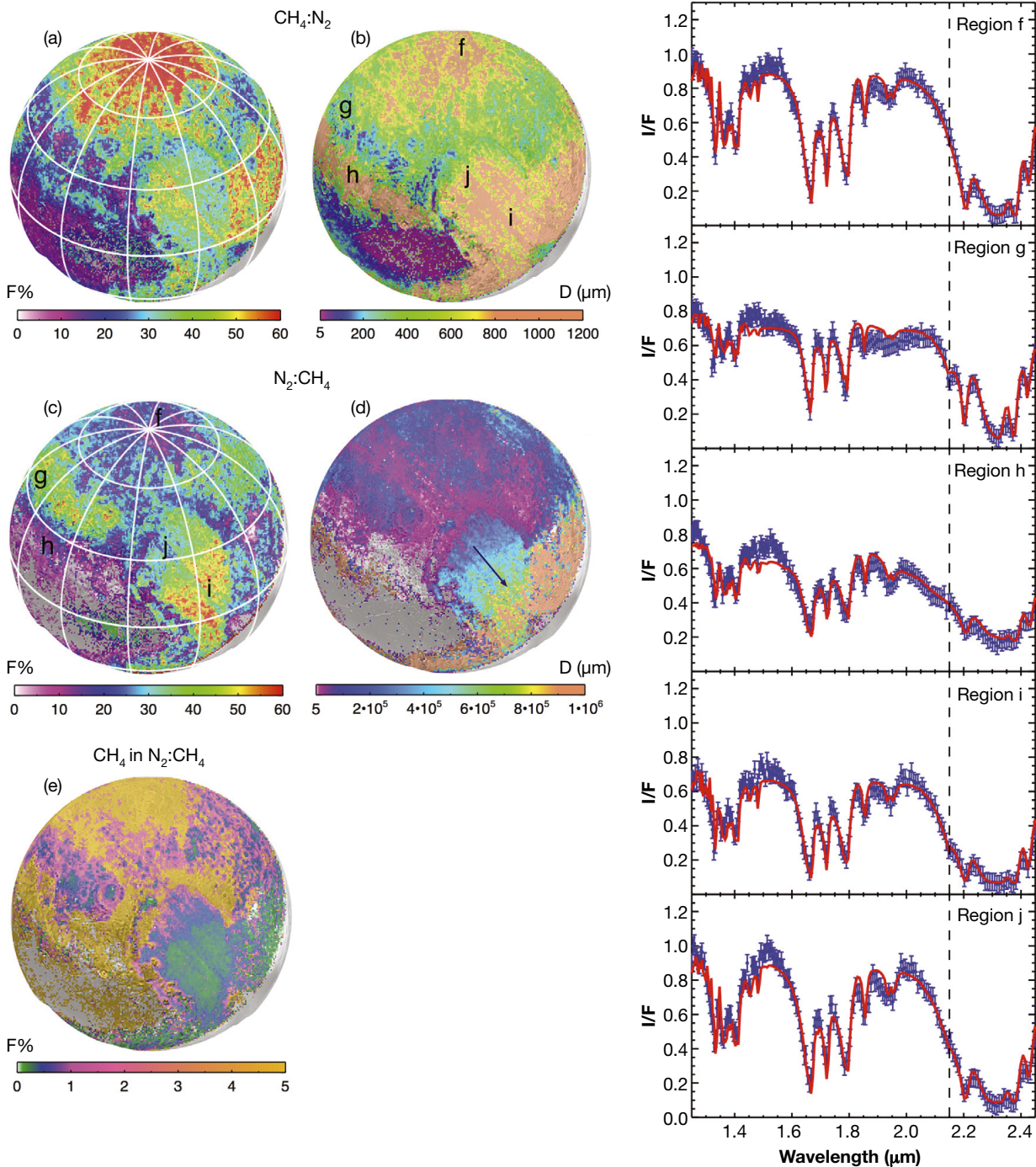


Figure 10. Pluto compositional maps obtained by applying a pixel-by-pixel Hapke radiative transfer model to the LEISA spectral images. CH_4 -rich component displaying (a) its relative abundance and (b) its relative path length. (c and d) The relative abundance and path length, respectively, of the N_2 -rich component. (e) The dilution fraction of CH_4 in N_2 . The composition maps are superimposed on the reprojected LORRI base map. Spectra extracted in regions of interest and labeled in (b and c) are shown as blue dots on the right-hand plots. The spectra are compared with their corresponding best-fit models (solid red line). (Reprinted from Protopapa et al.,¹² with permission from Elsevier, and Cruikshank et al.¹³)

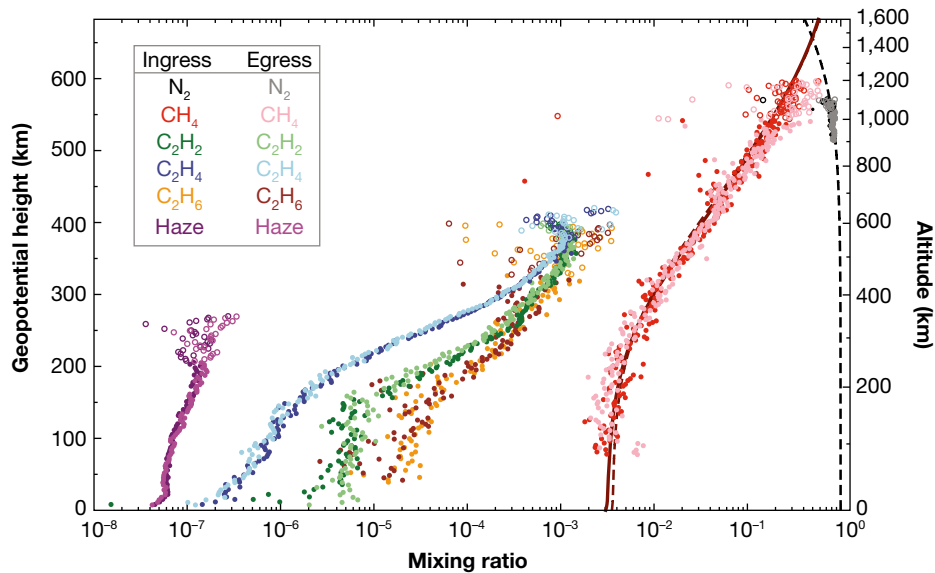


Figure 11. Mixing ratios versus geopotential height (left axis) and altitude (right axis) of various species detected in Pluto's atmosphere during solar occultation observations with the Alice ultraviolet spectrograph. For haze, the value plotted is $\epsilon \cdot 10^{15}/n_{\text{total}}$ where ϵ is the extinction coefficient in cm^{-1} . Solid and dashed lines are two models of CH_4 vertical transport. Open circles indicate where the uncertainty exceeds a factor of 2. (Adapted from Stern et al.⁴ and Young et al.,¹⁴ with permission from Elsevier.)

Similar maps can be constructed showing the distribution of CO and H_2O . Even though it probably composes most of Pluto's mantle, H_2O had not previously been detected on Pluto's surface because CH_4 absorptions dominate the spectra obtained from Earth. NH's superb spatial resolution was needed to locate the handful of H_2O -rich regions on Pluto's surface.

At the very cold temperatures on Pluto's surface (~ 40 K), H_2O behaves more like rock than ice. But there is indirect evidence that H_2O may exist in liquid form beneath a mantle of solid H_2O (mixed with rock), producing a globally distributed ocean on Pluto. Models of Pluto's interior suggest strong differentiation from the surface to the core (similar to other planets in the solar system), and thermodynamic arguments further suggest that a deep layer of liquid water could be stable beneath Pluto's icy crust. The near-alignment of SP with the sub-Charon point is perhaps additional evidence for a subsurface ocean, if SP experienced true polar wander that moved the original location of the impact basin to its current location. A Pluto orbiter mission is likely needed to determine whether Pluto is truly an ocean world.

Just like on Earth, Pluto's atmosphere is dominated by N_2 gas, although the surface pressure at Pluto is roughly 100,000 times lower than Earth's (~ 10 μbar for Pluto versus 1 bar for Earth). NH's Radio Science Experiment (REX) instrument measured the density and temperature of Pluto's lower atmosphere as a function of height using a unique radio occultation experiment in which powerful (~ 80 kW) beams of X-band radiation were directed at NH's 2.1-m antenna by the 70-m Earth-based antennas of NASA's Deep Space Network during NH's passage into (ingress) and out of (egress) Pluto's shadow. The REX data were processed to obtain Pluto's surface pressure definitively for the first time, while also showing that the temperature at high altitudes (>900 km) was

much colder than expected (~ 65 – 70 K), which explained why the atmospheric escape rate was ~ 10 – 100 times smaller than predicted by pre-encounter models.

The data from an ultraviolet solar occultation experiment conducted by the Alice instrument nearly simultaneously with the REX occultation were used to derive mixing ratios (i.e., relative abundances) as a function of altitude for N_2 , CH_4 , C_2H_2 , C_2H_4 (ethylene), and C_2H_6

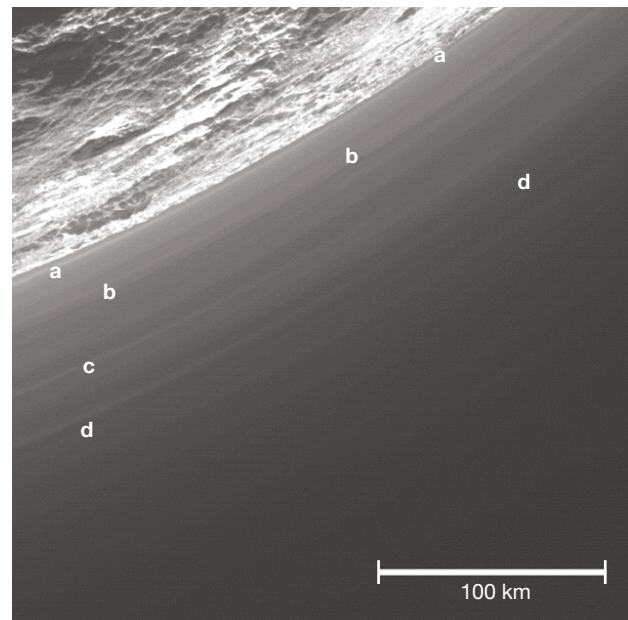


Figure 12. Pluto's atmosphere has highly structured aerosol haze layers. In the LORRI image above, taken at a solar phase angle of 147° , the haze extends from near the surface to an altitude >200 km. The haze layers (a) change thickness horizontally, (b) merge or split, (c) appear and disappear. (d) A dark lane at 72 km altitude is near the minimum of the atmospheric buoyancy frequency. (Adapted from Stern et al.⁴ and Cheng et al.,¹⁵ with permission from Elsevier.)

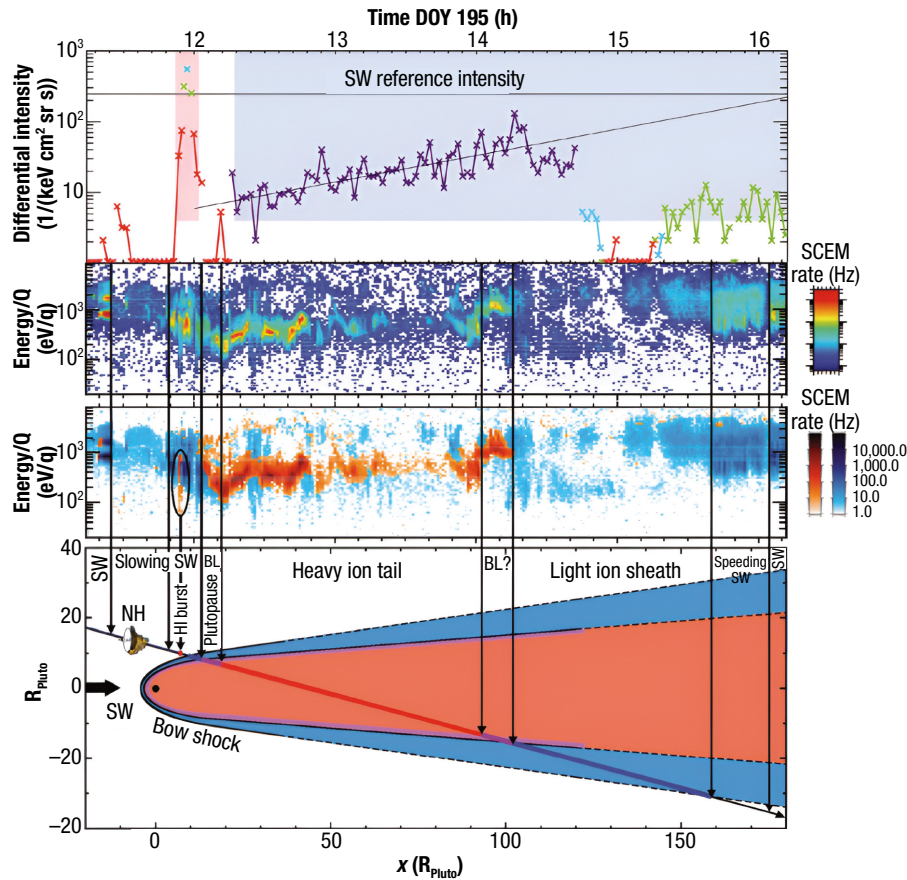


Figure 13. Overview of plasma data taken during the NH flyby of Pluto. (Top) PEPSSI data from Kollmann et al.¹⁶ The x symbols and colored solid lines show intensities dominated by 18-keV He⁺ ions. The color coding marks measurements at different cone angles relative to the Sun. The middle two panels show SWAP data from McComas et al.¹⁷ Color spectrograms of count rates (with >3 counts/sample) for secondary counts (top middle) and (bottom middle) light ions (blue) from the solar wind (SW) and heavy ions (red) from Pluto. The bottom panel is a schematic diagram identifying the NH trajectory and key regions of the interaction: bow shock, light ion sheath (blue), heavy ion tail (red), and Plutopause boundary layer (BL, purple). The x coordinate is along the Sun–Pluto line, and the transverse distance is measured in the plane of x and the spacecraft’s trajectory, which is close to the ecliptic plane. A heavy ion burst was seen ahead of the shock when NH turned so that SWAP was viewing in the right direction to see newly ionized material starting to be picked up. (Adapted from Bagenal et al.¹⁸)

(ethane), while also measuring extinction by Pluto’s extensive haze layer (Figure 11). The haze layer was mapped by NH’s optical cameras (LORRI and MVIC) when they looked back toward the solar direction after Pluto CA and when the haze was lit up by scattering of solar light (Figure 12). The haze preferentially scatters light in the forward direction and is blue in color, consistent with 0.5- μm spherical particles near the surface and 0.4- to 1.0- μm fractal aggregates assembled from 10- to 20-nm monomers at an altitude of ~ 45 km. The extensive layering seen in the haze has been attributed to orographic gravity waves.¹⁵

During the Pluto flyby, the in situ plasma instruments (Pluto Energetic Particle Spectrometer Science Investigation, or PEPSSI; and Solar Wind Around Pluto, or SWAP) were used to constrain mass loading from the escaping gas from Pluto’s atmosphere (Figure 13), which produced a CH₄⁺ obstacle to the solar wind at $\sim 2.5 R_p$ (R_p is Pluto’s radius) on the sunward side, a bow shock $\sim 4.5 R_p$ sunward of Pluto, and a long CH₄⁺ tail ($>100 R_p$) down which $\sim 1\%$ of the escaping gas travels. Some of this escaping gas reaches Charon and may be responsible for Charon’s dark red pole, as discussed further below. The radio occultation data were also used to derive an upper electron density limit of $\sim 1,000 \text{ e/cm}^3$ for Pluto’s ionosphere.

Charon and the Small Satellites

NH data showed Charon to be very different from Pluto (Figure 14) but also intriguing, with a surface dominated by water ice, chasms much larger than Arizona’s Grand Canyon circling its equator, and reddish polar hoods. The giant chasms encircling Charon’s equator (Mandjet Chasma and Serenity Chasma; Figure 15) were likely produced shortly after the giant collision that produced the Pluto–Charon primary (i.e., over 4 billion years ago), when what was initially liquid water froze and expanded, causing extensional faults in the bedrock ice along Charon’s equator. The polar hoods (Mordor Macula at the north pole; Figure 15) were likely produced by the capture of methane molecules escaping from Pluto, which were gravitationally focused onto Charon where they condensed on the coldest regions near the poles and were then irradiated by solar H Lyman- α photons, breaking the bonds in the methane ice to produce red organics. Figure 15 shows a high-resolution color image of Charon and a DEM, with a few of its most striking features marked. The smooth plains of Vulcan Planum are plausibly the site of extrusion of material from Charon’s interior early in its history (~ 4 billion years ago).

Pluto’s small satellites (Styx, Nix, Kerberos, and Hydra, in order of their distances from Pluto) were



Figure 14. Pluto and Charon. Both are displayed at their true relative sizes using identical color and intensity stretches to illustrate their differences. Pluto is approximately twice as large as Charon, its average surface brightness is approximately double that of Charon’s, and its surface is much more variegated. See the text for further discussion.

resolved for the first time by NH (Figure 15), and spectra of Nix and Hydra showed deep absorption bands of water ice (Figure 16). The orbital planes of all the small satellites are nearly coincident with Pluto’s equatorial plane, which strongly suggests that these bodies were not captured from the general Kuiper Belt population, but instead formed by agglomeration in a disk of material produced in the aftermath of the Charon-forming collision. This genesis scenario for the small satellites is further supported by their highly elongated shapes (which is consistent with agglomeration in a debris disk), their high geometric albedos (reflecting their icy compositions, which are likely the result of their formation in the icy mantle debris from the differentiated bodies that collided to form the Pluto–Charon binary); their albedos are roughly three times larger than for typical KBOs), and the high crater densities measured on the surfaces of Nix and Hydra (which constrain the surface ages to >4 billion years, consistent with formation shortly after the Pluto–Charon binary formed).

The Arrokoth Flyby

The NH spacecraft made its CA to Arrokoth on New Year’s Day 2019 (January 1, 2019) at a distance of only 3,538 km. NH observations revealed Arrokoth to be a

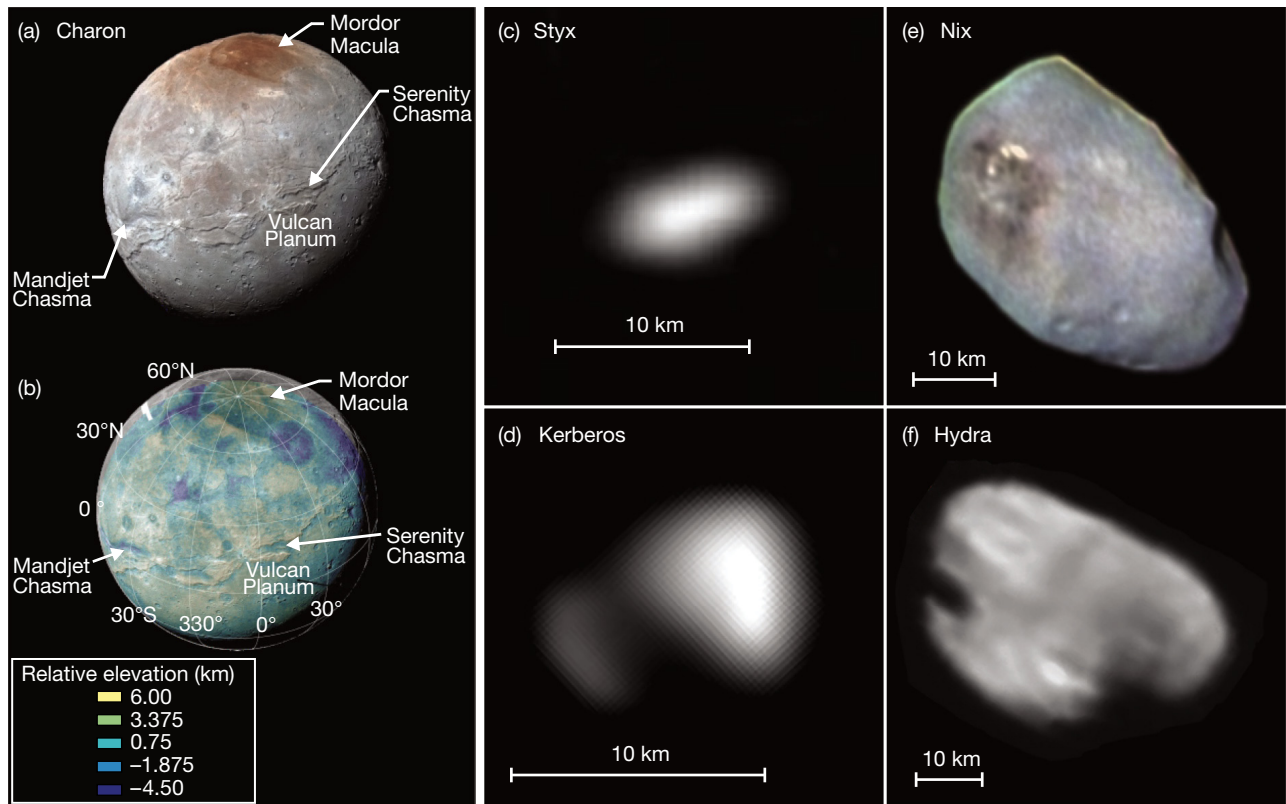


Figure 15. Images of Pluto’s satellites. (a) Enhanced NH color image of Pluto’s largest moon, Charon, with a few major regions of interest identified. (b) Digital terrain model of Charon showing the wide range of surface elevations. (c–f) Resolved images of Pluto’s four small moons taken during the NH flyby. (Adapted from Stern et al.⁴)

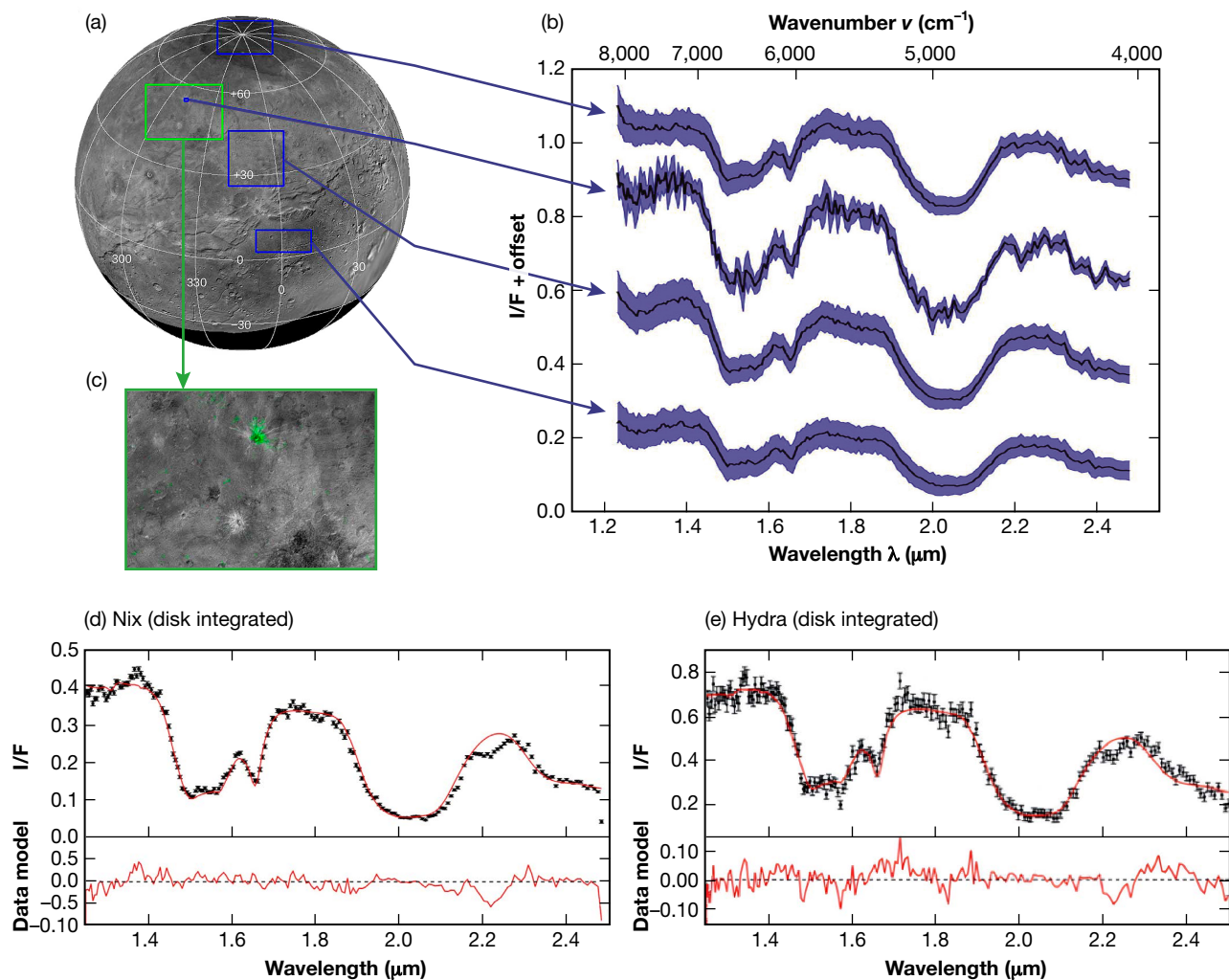


Figure 16. Spectra. (a) NH LORRI composite base map of Charon. LEISA near-infrared spectra were extracted from four different regions (green and blue boxes) and are plotted in panel (b). All four spectra show deep absorption bands centered near 1.5, 1.65, and 2 μm associated with crystalline water (H_2O) ice. However, the spectrum extracted from the region near Organa crater (green box, c) shows additional absorption near 2.22 μm associated with ammonia-bearing (NH_3 -bearing) species. Disk-integrated LEISA spectra of Nix (d) and Hydra (e) also show the deep absorption bands of crystalline water ice; the red curves in the upper portions of panels (d) and (e) are from model fits that include only crystalline H_2O ice. The plotted residuals (the red curves in the lower portions of the plots) show that both Nix and Hydra have an additional absorption feature near 2.2 μm , which may be associated with the same NH_3 -bearing species seen in the Organa crater on Charon. I/F, irradiance/solar flux. (Composite figure adapted from Stern et al.⁴ Panels a–c adapted from Grundy et al.,¹⁹ with permission from AAAS, and panels d and e from Cook et al.,²⁰ with permission from Elsevier.)

contact binary with two highly flattened lobes and a red, organic-rich surface (Figure 17) showing traces of methanol (CH_3OH) ice but essentially devoid of water ice. Arrokoth's longest dimension is only ~ 36 km, and it is testimony to NH's excellent navigation team that such a small body nearly 6.5 billion kilometers from Earth could be accurately targeted.

The KBOs are subdivided into several families depending on their orbital characteristics (e.g., inclination angle versus semimajor axis, as shown in Figure 18). Pluto falls into one of the families whose orbits are in mean motion resonances with Neptune (the 3:2 resonance for Pluto because its orbital period is exactly

1.5 times longer than Neptune's). Arrokoth is in the cold classical family whose members have orbital inclinations within 5° of the ecliptic plane and whose orbital eccentricities are smaller than 0.1. The cold classical KBOs are thought to be the least evolved (i.e., most primitive) bodies because they likely formed very close to their current heliocentric locations and have remained there for the past 4.5 billion years. KBOs in the scattered family have orbits that are strongly perturbed by gravitational interactions with Neptune. Some of the scattered KBOs, the so-called Centaurs, are perturbed into orbits that pass through the region containing the giant planets (Neptune, Uranus, Saturn, and Jupiter), where some

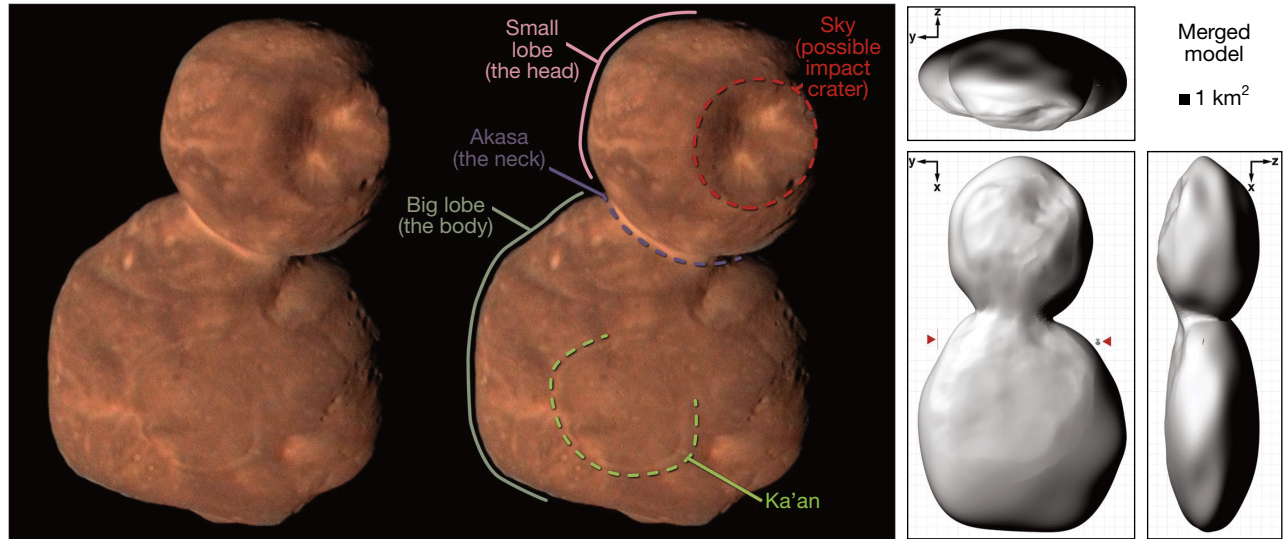


Figure 17. Arrokoth. Left, Highest-resolution view of (486958) Arrokoth. The image combines low-resolution, enhanced-color data (close to what the human eye would see) acquired by the NH MVIC instrument with high-resolution panchromatic data acquired by the NH LORRI instrument. The left-hand side of the figure shows the unannotated image, while the right-hand side has annotations labeling key features of Arrokoth, including the two lobes, the bright neck (named Akasa), the large crater on the small lobe (named Sky), and the annulus of bright material on the large lobe (named Ka'an). Right, Merged shape model, created by stitching a stereo shape model on a global shape model. The red arrow on the left side of the yx projection of Arrokoth's shape model points to a line segment the size of the Golden Gate Bridge in San Francisco (2 km), while the red arrow on the right side pointing to a line segment the size of the USS Enterprise (NCC-1701-D; 643 m). (Adapted from Keane et al.,²¹ CC BY-NC 4.0.)

eventually become the Jupiter-family comets (JFCs, like 67P/Churyumov-Gerasimenko, the target of the Rosetta mission). Analysis of the Arrokoth data provides some of the first detailed evidence for the “pebble cloud collapse” streaming instability model of planetesimal formation in the solar nebula (Figure 19).

The Jupiter Flyby

Although the principal objective of the Jupiter flyby was a gravity assist to cut more than 3 years off the travel time to Pluto, NH used the opportunity to perform

exciting and unique scientific investigations of the Jovian system. The Jupiter flyby also served as an early rehearsal of the NH team's ability to conduct a systematic investigation of a planetary system that could inform the planning for the Pluto flyby much later in the mission. Indeed, the plans for the Jupiter flyby became so ambitious that the number of observations and the amount of data collected actually eclipsed what was originally planned, and laid out in the NH's proposal to NASA, for the Pluto system flyby. Amazingly, the Jupiter flyby was executed almost flawlessly, with only a few minor

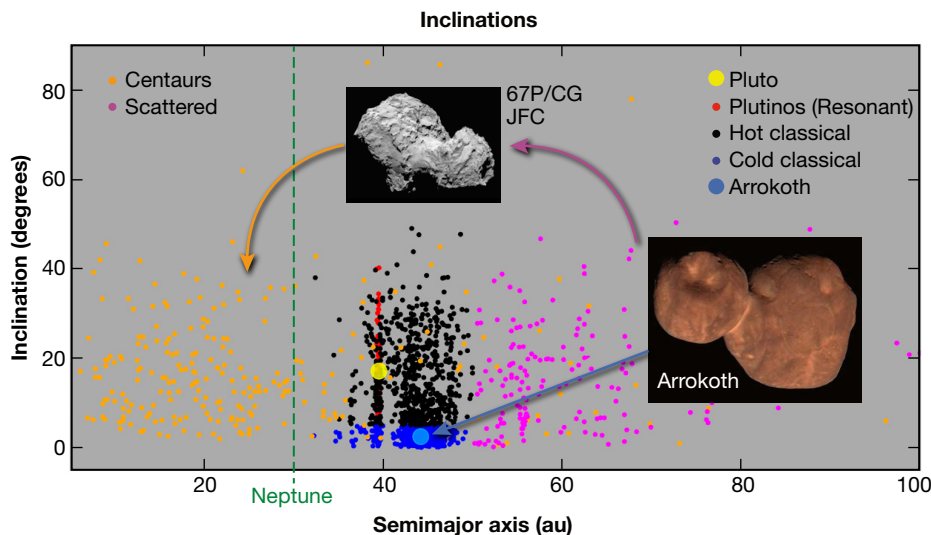


Figure 18. KBO families. Families are depicted by colored circles (each family is in one color), and the orbital inclination angle versus the semimajor axis is plotted. Arrokoth is in the cold classical family whose members are thought to be among the least evolved (i.e., most primitive) bodies in the solar system because they likely formed very close to their current heliocentric locations and have remained there for the past 4.5 billion years. See the text for further discussion.

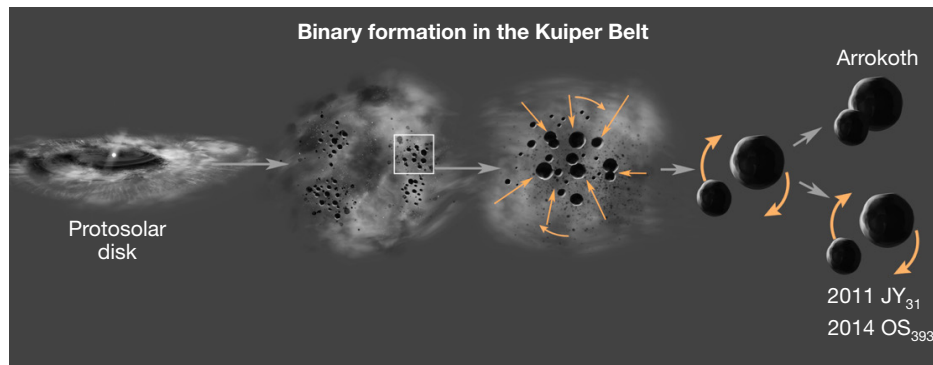


Figure 19. The NH results on Arrokoth support a streaming instability model for planetesimal formation in the outer solar system, in which rotating pebble clouds in the protosolar disk collapse to form kilometer-size bodies. Mutual gravitational interactions at relatively slow speeds (several kilometers per hour) usually result in either binary formation (as observed by NH for the two small KBOs 2011 JY₃₁ and 2014 OS₃₉₃; see the Cruise Science section) or subsequent merging of two bodies to form a bilobed object like Arrokoth.

glitches that served as lessons learned for the Pluto flyby (e.g., some Alice spectrograph parameters were set too conservatively, which shut down that instrument near the time of CA).

On February 28, 2007, at 05:43:40 UTC, the NH spacecraft made its CA to Jupiter at a distance of 2.3 million kilometers (1.4 million miles; 32 Jovian radii). The major scientific results from the Jupiter flyby included the following:

- Documenting morphological changes in Jupiter's belts and zones
- Providing high-resolution measurements and measuring wind speeds of a newly discovered "Little Red Spot"
- Measuring atmospheric waves in Jupiter's mesosphere
- Probing Jupiter's atmospheric composition at 256 wavelengths and detecting fresh reservoirs of ammonia clouds near the Great Red Spot
- Measuring powerful lightning strikes and auroral activity in the polar regions of Jupiter's atmosphere
- Detecting new structures in the Jovian dust rings
- Probing hydrocarbons in Jupiter's atmosphere via an ultraviolet (UV) stellar occultation
- Measuring UV auroral activity on Ganymede
- Conducting unprecedented monitoring of volcanic eruptions on Io
- Mapping Jupiter's massive magnetosphere all the way down its magnetotail

These results were reported in nine papers appearing in the October 12, 2007, issue of *Science* magazine. The cover of the issue (Figure 20) featured a color image of Io sprouting a gigantic volcanic plume next to a spectacular infrared spectral image of Jupiter. Highlights from LORRI imaging of the Jovian system are displayed in a separate montage (Figure 21).



Figure 20. *Science* magazine cover featuring NH (vol. 318, no. 5848, October 12, 2007). The NH flyby of Jupiter in February 2007 produced outstanding scientific results that were published in *Science* magazine. The cover featured a composite of a LEISA infrared spectral image of Jupiter and a LORRI image, colored by MVIC spectral data, of Io and its spectacular volcanic plumes.

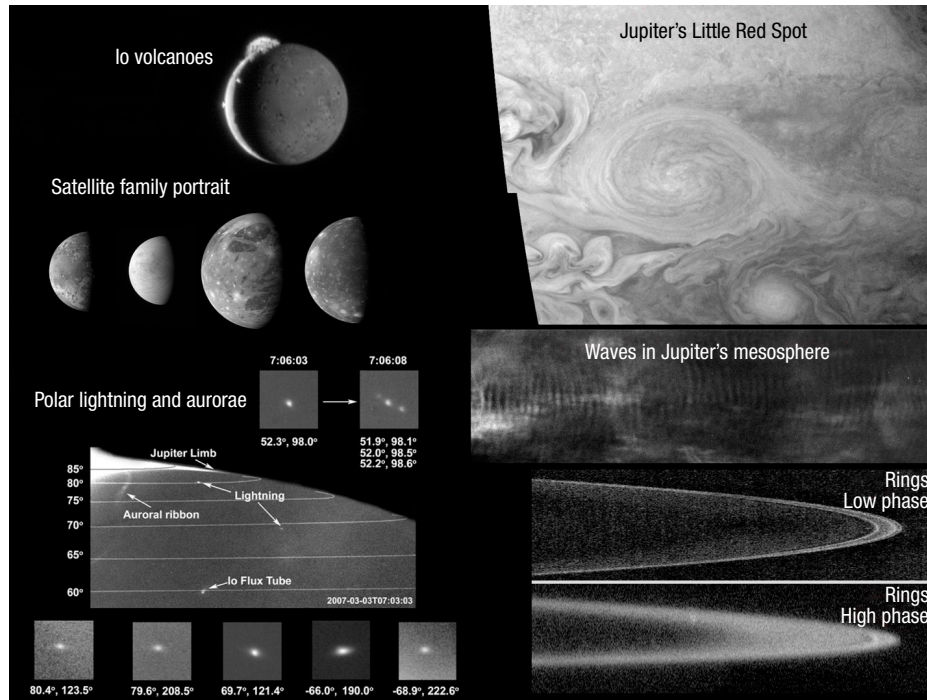


Figure 21. Highlights from LORRI imaging during the Jupiter flyby. Upper left, spectacular plumes from Io's volcanoes. Middle left, high-resolution imaging of all four Galilean satellites. Lower left, discovery of powerful lightning strikes at high polar latitudes and measurement of auroral features in Jupiter's atmosphere. Upper right, highest-resolution images ever of Jupiter's newly discovered Little Red Spot. Middle right, measurements of waves in Jupiter's mesosphere. Lower right, observations of new features in Jupiter's tenuous dust ring.

Cruise Science

Although there are large temporal gaps between NH's three close flybys, unique and exciting science was steadily collected during those gaps, constituting a rich cruise science phase of the mission. Even during spacecraft hibernations, in which most subsystems were shut down to conserve resources and simplify operations, NH had the capability to keep the plasma instruments (PEPSSI and SWAP) running to collect in situ data on the solar wind, suprathermal ions, and cosmic rays, which could be stored onboard and then transmitted to the ground when normal operations resumed. Figure 22 shows examples of PEPSSI and SWAP data obtained during the cruise science phase. In addition, the Venetia Burney Student Dust Counter (VBSDC) made its most sensitive measurements during hibernation phases, when it recorded dust impacts along NH's spacecraft trajectory surpassing what had been captured in previous dust measurements once NH moved past Saturn's orbit. Figure 23 shows the VBSDC dust impact results through July 2022 when the spacecraft's heliocentric distance was 53 au. VBSDC measurements are not only providing the first-ever data on the dust environment in the Kuiper Belt, but they will also constrain the properties of a putative outer Kuiper Belt extending out to ~110 au.

In addition to the plasma and dust measurements, LORRI and MVIC also collected unique science data during multiple three-axis periods during the cruise phase. LORRI observed three other dwarf planets (i.e., in addition to Pluto and Charon), four other large (diameters > 300 km) KBOs, and 26 smaller KBOs (including Arrokoth). Unlike Earth-based KBO observations, which are generally limited to phase angles of 2°, LORRI conducted observations of many its KBO targets over a wide range of solar phase angles (~

solar phase curves (i.e., brightness as a function of solar phase angle), the NH team showed that the brightnesses of the small KBOs decrease much faster with increasing phase than observed for the larger KBOs, which can plausibly be attributed to the small KBOs having rougher surfaces compared with the smooth icy surfaces on the larger bodies.

LORRI's extensive temporal monitoring of KBO brightnesses was also used to constrain the KBO shapes and rotational states. The NH data showed that the rotational poles of the small KBOs generally had large obliquities (i.e., the pole directions made large angles to the KBO orbital plane around the Sun), and these KBOs were likely either highly elongated or double-lobed objects, similar to what was found for Arrokoth, which suggests a primordial origin for their rotational properties that helps to constrain how planetesimals formed within the solar nebula. While the small KBOs observed during KEM1 were dominated by cold classical objects, similar investigations of hot classicals and scattered disk KBOs in KEM2 can be used to determine whether these findings extend to the other KBO populations, lending additional insights into planetesimal formation scenarios.

The NH spacecraft passed within 0.3 au of five KBOs (four cold classical KBOs and one scattered KBO), enabling sensitive searches for potential companions.

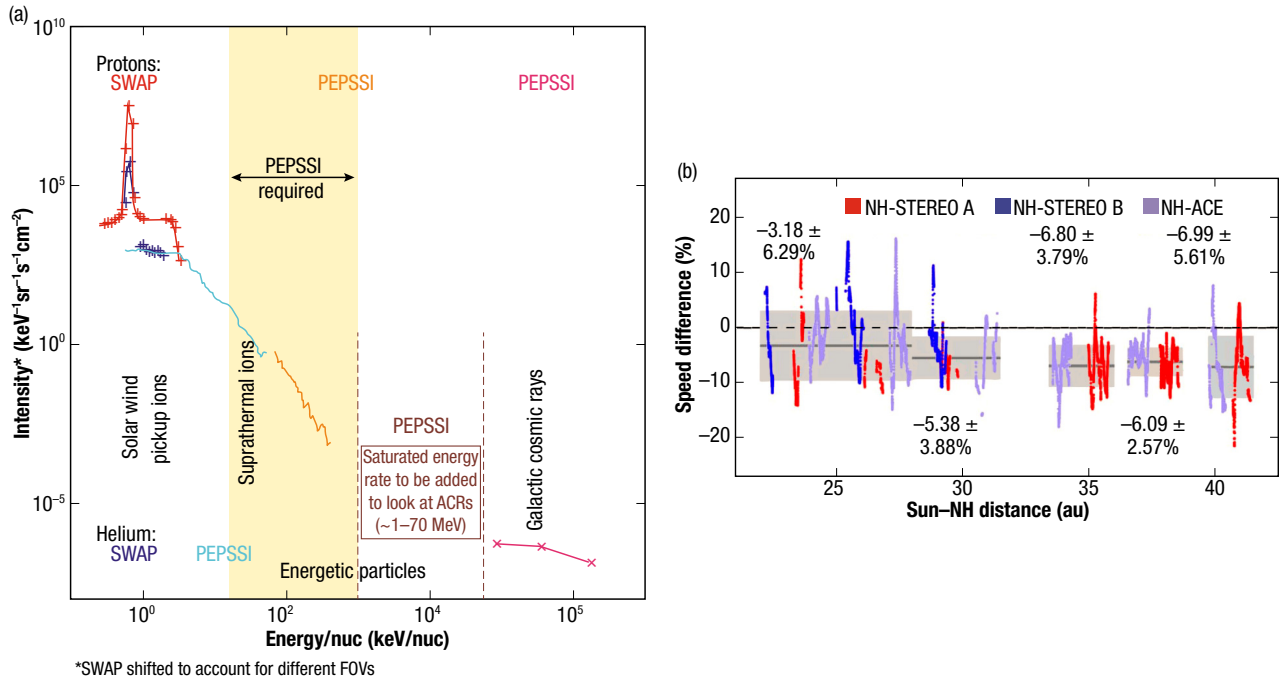


Figure 22. PEPSSI and SWAP data obtained during the cruise science phase. Left, overview of particle spectrum showing the proton and helium measurements from NH, composed of solar wind and interstellar pickup ions from SWAP (at the lowest energies) and pickup ions, suprathermal ions, and cosmic rays from PEPSSI. In KEM2, PEPSSI is adding measurements of 1- to 70-MeV H, He, and O particles to fill in a gap in the earlier data. Right, SWAP data show a marked decrease in the speed of the solar wind at heliocentric distances >20 au compared with measurements made by Solar TERrestrial RELations Observatory (STEREO)-A, STEREO-B, and Advanced Composition Explorer (ACE) near 1 au (using data from those three instruments taken from solar longitudes within 45° of NH's value), possibly associated with increased loading of solar wind by interstellar particles at larger heliocentric distances. (Panel b reproduced from Elliott et al.²² by permission of the AAS.)

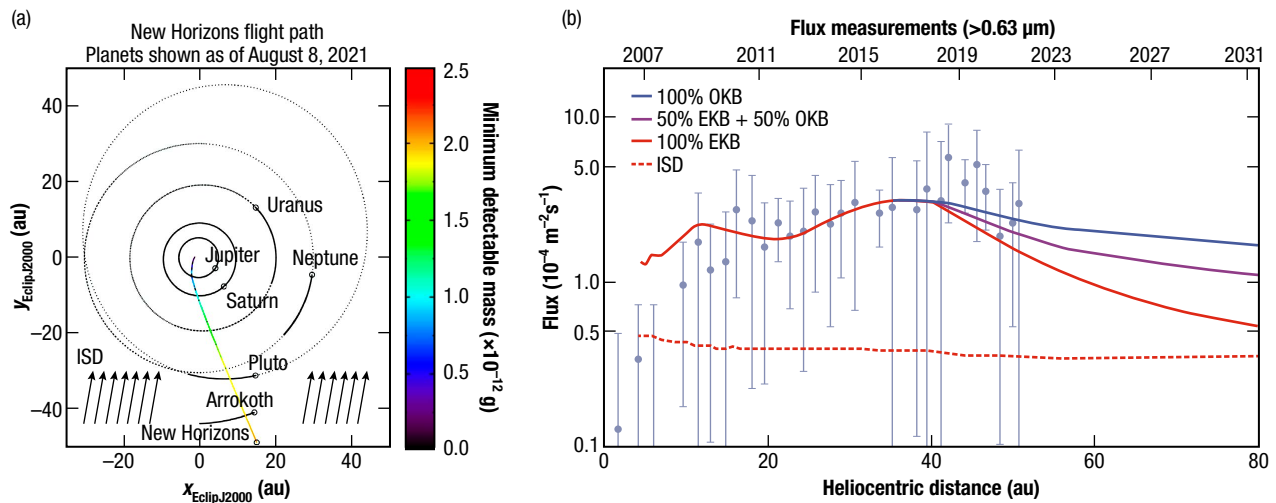


Figure 23. VBSDC dust impact results through July 2022. (a) The trajectory of NH past 50 au. The decrease in spacecraft speed with increasing distance results in a higher minimum detectable mass, as indicated by the color coding. NH is now heading along an ecliptic longitude $\lambda_{NH} = 293^\circ$ (the ecliptic plane contains Jupiter and the Sun and most of the planets) compared with the interstellar dust (ISD) inflow of $\lambda_{ISD} \approx 259^\circ$, indicated by the parallel upward-pointing arrows at the bottom of the plot. (b) Plot of the estimated dust flux onto VBSDC for grains with interplanetary dust particle (IDP) radii > 0.63 μm . The three curves are models^{23,24} fitted to VBSDC measurements assuming only Kuiper Belt distribution (red), a putative outer Kuiper Belt distribution with initial semimajor axes between 80 and 110 au (blue), and a combination of the two with equal weight (purple). Future VBSDC measurements will constrain these models. (Adapted from Bernardoni, Horányi, and Doner,²⁵ CC BY 4.0.)

LORRI definitively detected a companion around one of its nearby KBO targets (the cold classical 2011 JY₃₁) and likely detected a companion around another one (the cold classical 2014 OS₃₉₃), which supports the hypothesis that up to two-thirds of the cold classical KBOs are binaries (one of the cold classical KBOs was too faint to provide useful binary constraints). And MVIC performed color observations of both Uranus and Neptune at high-solar-phase angles, providing important new information on the scattering properties of the hazes of those ice giants for comparison with the data from the Voyager flybys in the late 1980s, the last time similar observations were made.

SUMMARY

NH was the first in a new (in 2002) series of NASA principal investigator–led midsize planetary missions that are intermediate in budget and scientific scope between Discovery-class and Flagship missions. After its launch in January 2006, NH successfully executed three close flybys (Jupiter, Pluto, and Arrokoth) and has revolutionized our understanding of the Pluto system and the Kuiper Belt. NH transformed our view of Pluto from a barely resolved astronomical object to a vibrant world with incredible surface complexity and diversity and with different climate zones driven by a fascinating hazy atmosphere. NH similarly revealed exciting new details on Pluto’s five moons (including its binary twin Charon, as well as Styx, Nix, Kerberos, and Hydra). The detailed NH investigation of the small KBO Arrokoth, likely the most primitive object ever visited by a spacecraft, has provided the first direct evidence supporting the streaming instability model of planetesimal formation in the early solar system. NH also provided exciting and unique scientific results on the solar wind, the interplanetary particle and dust environment, and other dwarf planets and KBOs during its cruise and hibernation phases. Given that its instruments and spacecraft are still as capable as they were at launch more than 17 years ago, the NH mission is continuing its exploration of the outer solar system and heliosphere and should be able to do so for many more years.

ACKNOWLEDGMENTS: Work on the New Horizons mission was performed under NASA contracts NAS5-97271/TO30 (APL) and NASW-02008 (SwRI).

REFERENCES

- ¹S. A. Stern, “The New Horizons Pluto Kuiper Belt mission: An overview with historical context,” *Space Sci. Rev.*, vol. 140, pp. 3–21, 2008, <https://doi.org/10.1007/s11214-007-9295-y>.
- ²National Research Council. *New Frontiers in Solar System Exploration*. Washington, DC: National Academies Press, 2003, <https://doi.org/10.17226/10898>.
- ³S. A. Stern, J. M. Moore, W. M. Grundy, L. A. Young, and R. P. Binzel, Eds., *The Pluto System after New Horizons*. Tucson, AZ: Univ. of Arizona Press, 2021.
- ⁴S. A. Stern, W. M. Grundy, W. B. McKinnon, H. A. Weaver, and L. A. Young, “The Pluto system after New Horizons,” *Annu. Rev. Astron. Astrophys.*, vol. 56, pp. 357–392, 2018, <https://doi.org/10.1146/annurev-astro-081817-051935>.
- ⁵J. M. Moore and W. B. McKinnon, “Geologically diverse Pluto and Charon: Implications for the dwarf planets of the Kuiper Belt,” *Ann. Rev. Earth Planet. Sci.*, vol. 49, pp. 173–200, 2021, <https://doi.org/10.1146/annurev-earth-071720-051448>.
- ⁶G. R. Gladstone and L. A. Young, “New Horizons observations of the atmosphere of Pluto,” *Ann. Rev. Earth Planet. Sci.*, vol. 47, pp. 119–140, 2019, <https://doi.org/10.1146/annurev-earth-053018-060128>.
- ⁷S. A. Stern, H. A. Weaver, J. R. Spencer, and H. A. Elliott, and the New Horizons team, “The New Horizons Kuiper Belt Extended Mission,” *Space Sci. Rev.*, vol. 214, no. 4, art. 77, 2018, <https://doi.org/10.1007/s11214-018-0507-4>.
- ⁸S. A. Stern, J. R. Spencer, H. A. Weaver, and C. B. Olkin, “The exploration of the primordial Kuiper Belt Object Arrokoth (2014 MU69) by New Horizons,” in *The Pluto System after New Horizons*, S. A. Stern, J. M. Moore, W. M. Grundy, L. A. Young, R. P. Binzel, Eds., Tucson, AZ: Univ. of Arizona, 2021, pp. 587–601, https://doi.org/10.2458/azu_uapress_9780816540945-ch025.
- ⁹NASA, “Pluto Kuiper Belt mission announcement of opportunity,” AO 01-OSS-01, Jan. 19, 2001.
- ¹⁰O. L. White, J. M. Moore, A. D. Howard, P. M. Schenk, K. N. Singer, D. A. Williams, and R. M. C. Lopes, “The geology of Pluto,” in *The Pluto System after New Horizons*, S. A. Stern, J. M. Moore, W. M. Grundy, L. A. Young, R. P. Binzel, Eds., Tucson, AZ: Univ. of Arizona, 2021, pp. 55–87, https://doi.org/10.2458/azu_uapress_9780816540945-ch004.
- ¹¹C. B. Olkin, C. J. A. Howett, S. Protopapa, W. M. Grundy, A. J. Verbiscer, and M. W. Buie, “Colors and photometric properties of Pluto,” in *The Pluto System after New Horizons*, S. A. Stern, J. M. Moore, W. M. Grundy, L. A. Young, R. P. Binzel, Eds., Tucson, AZ: Univ. of Arizona, 2021, pp. 147–163, https://doi.org/10.2458/azu_uapress_9780816540945-ch008.
- ¹²S. Protopapa, W. M. Grundy, D. C. Reuter, D. P. Hamilton, C. M. Dalle Ore, et al., “Pluto’s global surface composition through pixel-by-pixel Hapke modeling of New Horizons Ralph/LEISA data,” *Icarus*, vol. 287, pp. 218–228, 2017, <https://doi.org/10.1016/j.icarus.2016.11.028>.
- ¹³D. P. Cruikshank, W. M. Grundy, S. Protopapa, B. Schmitt, and I. R. Linscott, “Surface composition of Pluto,” in *The Pluto System after New Horizons*, S. A. Stern, J. M. Moore, W. M. Grundy, L. A. Young, R. P. Binzel, Eds., Tucson, AZ: Univ. of Arizona, 2021, pp. 55–87, https://doi.org/10.2458/azu_uapress_9780816540945-ch009.
- ¹⁴L. A. Young, J. A. Kammer, A. J. Steffl, G. R. Gladstone, M. E. Summers, et al., “Structure and composition of Pluto’s atmosphere from the New Horizons solar ultraviolet occultation,” *Icarus*, vol. 300, pp. 174–199, 2018, <https://doi.org/10.1016/j.icarus.2017.09.006>.
- ¹⁵A. F. Cheng, M. F. Summers, G. R. Gladstone, D. F. Strobel, L. A. Young, et al., “Haze in Pluto’s atmosphere,” *Icarus*, vol. 290, pp. 112–133, 2017, <https://doi.org/10.1016/j.icarus.2017.02.024>.
- ¹⁶P. Kollmann, M. E. Hill, R. C. Allen, R. L. McNutt Jr., L. E. Brown, et al., “Pluto’s interaction with energetic heliospheric ions,” *JGR Space Phys.*, vol. 124, no. 9, pp. 7413–7424, 2019, <https://doi.org/10.1029/2019JA026830>.
- ¹⁷D. J. McComas, H. A. Elliott, S. Weidner, P. Valek, E. J. Zirnstein, et al., “Pluto’s interaction with the solar wind,” *JGR Space Phys.*, vol. 121, no. 5, pp. 4232–4246, 2016, <https://doi.org/10.1002/2016JA022599>.
- ¹⁸F. Bagenal, D. J. McComas, H. A. Elliott, E. J. Zirnstein, R. L. McNutt Jr., et al., “Solar wind interaction with the Pluto system,” in *The Pluto System after New Horizons*, S. A. Stern, J. M. Moore, W. M. Grundy, L. A. Young, R. P. Binzel, Eds., Tucson, AZ: Univ. of Arizona, 2021, pp. 379–392, https://doi.org/10.2458/azu_uapress_9780816540945-ch016.
- ¹⁹W. M. Grundy, R. P. Binzel, B. J. Buratti, J. C. Cook, D. P. Cruikshank, et al., “Surface compositions across Pluto and Charon,” *Science*, vol. 351, no. 6279, pp. aad9189-1–aad9189-8, 2016, <https://doi.org/10.1126/science.aad9189>.

- ²⁰J. A. Cook, C. M. Dalle Ore, S. Protopapa, R. P. Binzel, R. Cartwright, et al., "Composition of Pluto's small satellites: Analysis of New Horizons spectral images," *Icarus*, vol. 315, pp. 30–45, 2018, <https://doi.org/10.1016/j.icarus.2018.05.024>.
- ²¹J. T. Keane, S. B. Porter, R. A. Beyer, et al., "The geophysical environment of (486958) Arrokoth—A small Kuiper Belt object explored by New Horizons," *JGR Planets*, vol. 127, no. 6, art. e2021JE007068, 2022, <https://doi.org/10.1029/2021JE007068>.
- ²²H. A. Elliott, D. J. McComas, E. J. Zirnstein, B. M. Randol, P. A. Delamere, et al., "Slowing of the solar wind in the outer heliosphere," *Astrophys. J.*, vol. 885, art. 156, 2019, <https://doi.org/10.3847/1538-4357/ab3e49>.
- ²³A. R. Poppe, "An improved model for interplanetary dust fluxes in the outer Solar System," *Icarus*, vol. 264, pp. 369–386, 2016, <https://doi.org/10.1016/j.icarus.2015.10.001>.
- ²⁴A. R. Poppe, C. M. Lisse, M. Piquette, M. Zemcov, M. Horányi, et al., "Constraining the Solar System's debris disk with in situ New Horizons measurements from the Edgeworth-Kuiper Belt," *Astrophys. J. Lett.*, vol. 881, art. L12, 2019, <https://doi.org/10.3847/2041-8213/ab322a>.
- ²⁵E. Bernardoni, M. Horányi, A. Doner, M. Piquette, J. R. Szalay, et al., "Student Dust Counter status report: The first 50 au," *Planet. Sci. J.*, vol. 3, art. 69, 2022, <https://doi.org/10.3847/PSJ/ac5ab7>.



Harold A. Weaver, Space Exploration Sector, Johns Hopkins University Applied Physics Laboratory, Laurel, MD

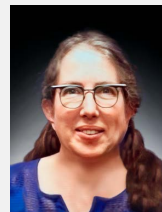
Harold A. Weaver is a scientist in APL's Space Exploration Sector. He received a BS in physics from Duke University and an MS and a PhD in physics from Johns Hopkins University. Hal was the project scientist on NASA's New Horizons mission during 2003–2022 and the principal investigator (PI) of NH's Long Range Reconnaissance Imager (LORRI) during 2016–2022, and he has been a New Horizons science co-investigator (CoI) since 2003. He also served as the PI of the LORRI instrument on NASA's Lucy mission from 2017 to 2022. He has been pursuing space-borne, rocket-borne, and ground-based investigations in planetary science since 1978. Hal received the NASA Medal for Exceptional Scientific Achievement in 1988 for his role in discovering water emissions from Comet Halley using NASA's Kuiper Airborne Observatory. He has led multiple investigations of comets using the International Ultraviolet Explorer, the Hubble Space Telescope, and the Far Ultraviolet Spectroscopic Explorer, and he was a CoI on the Rosetta-Alice instrument. In 2005, Hal co-led the team that discovered two small satellites of Pluto (Nix and Hydra). He is a fellow of the American Astronomical Society and a full member of the International Academy of Astronautics. His email address is hal.weaver@jhuapl.edu.



S. Alan Stern, Southwest Research Institute, Boulder, CO

S. Alan Stern is the associate vice president of Southwest Research Institute's space sector. He has an MS in atmospheric sciences from the University of Texas, an MS in aerospace engineering from the University of Texas, and a PhD in astrophysics and planetary science from the University of Colorado. In 2020, NASA appointed Alan to fly to space as a researcher aboard a commercial suborbital space mission. He formerly served as NASA's chief of space and Earth science programs. His career has taken him to numerous observatories, the South Pole, the Titanic, and the upper atmosphere aboard high-performance NASA aircraft. He has served on 29 space missions. He is a member of the US National Science Board and leads NASA's New Horizons mission to Pluto and the Kuiper Belt as its principal investigator. He has published over 440 technical papers and written three books. He is an associate fellow of the American Institute of Aeronautics and Astronautics (AIAA) and a fellow of the American Association for the Advancement of Science (AAAS), the Royal Astronomical Society (RAS), the American Geophysical Union (AGU), and the Explorer's Club. He was awarded the von Braun Aerospace Achievement

Award, *Smithsonian Magazine's* American Ingenuity Award, American Astronautical Society's Sagan Memorial Award, and NASA's Distinguished Public Service Medal. In both 2007 and 2016, he was named to the Time 100. His email address is astern@swri.org.



Leslie A. Young, Southwest Research Institute, Boulder, CO

Leslie A. Young is a staff scientist in the Solar System Science and Exploration Division of the Southwest Research Institute. She received a BA in physics from Harvard University and a PhD in earth, atmospheric, and planetary sciences from the Massachusetts Institute of Technology (MIT). Leslie was the deputy project scientist on NASA's New Horizons mission during 2003–2017 and the lead on the Pluto encounter planning 2003–2015, and she has been a New Horizons science co-investigator since 2003. She has been studying Pluto's surface and atmosphere, and other tenuous atmospheres, since 1987. In 1988, Leslie was a member of the team that discovered Pluto's atmosphere. She is a fellow of the American Astronomical Society and a full member of the International Academy of Astronautics. Asteroid 17242 Lesliyoung (2000 EX130) was named in her honor. Her email address is leslie.young@swri.org.



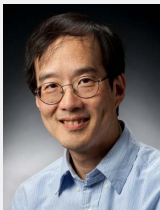
John R. Spencer, Southwest Research Institute, Boulder, CO

John R. Spencer is an institute scientist in Southwest Research Institute's Department of Space Studies. He obtained a BS in geology from the University of Cambridge and a PhD in planetary sciences from the University of Arizona. He specializes in studies of the moons of the outer planets, particularly the four large "Galilean" satellites of Jupiter, and other small outer-solar-system bodies, using theoretical models, Earth-based telescopes, close-up spacecraft observations, and the Hubble Space Telescope. John is a New Horizons science team member and a deputy project scientist for its extended mission into the Kuiper Belt. He coordinated the search for Kuiper Belt object (KBO) flyby targets beyond Pluto, which led to the discovery of New Horizons' next target, the small KBO Arrokoth. He also led New Horizons' search, during Pluto approach, for potential debris hazards in the Pluto system and led the science planning of the successful 2019 flyby of Arrokoth. In 2016 he won the American Geophysical Union (AGU) Whipple Award for "outstanding contributions in the field of planetary science," and in 2021 he was elected a fellow of the AGU. His email address is spencer@boulder.swri.edu.



Catherine B. Olkin, Muon Space, Mountain View, CA

Catherine B. Olkin is a scientist at Muon Space. She received a BS in aeronautics and astronautics from the Massachusetts Institute of Technology (MIT), an MS in aeronautics and astronautics from Stanford University, and PhD in earth, atmospheric, and planetary sciences from MIT. Cathy was the deputy project scientist on NASA's New Horizons mission, the principal investigator of New Horizons' Ralph instrument (a color camera and infrared imaging spectrometer), and a New Horizons science co-investigator (CoI). She has investigated planetary atmospheres and surfaces using both ground-based and space-based observations. She was the deputy principal investigator for NASA's Lucy mission to the Jupiter Trojan asteroids during its development, and she continues as a CoI on the Lucy mission. Currently, Cathy is a principal scientist at Muon Space and leads an effort to develop a constellation of satellites to detect wildfires early across the globe and provide high-spatial-resolution, timely data to first responders. Her email address is cathy@muonspace.com.



Andrew F. Cheng, Space Exploration Sector, Johns Hopkins University Applied Physics Laboratory, Laurel, MD

Andrew F. Cheng is the chief scientist in APL's Space Exploration Sector. He has a BA from Princeton University and an MS and a PhD from Columbia University, all in physics. As chief scientist, he is the sector's external liaison for space science and provides independent science advice and strategic vision to APL and sector leadership. He is a member of the MESSENGER (MERcury Surface, Space ENVIRONMENT, GEOchemistry, and Ranging) science team and principal investigator for the Long Range Reconnaissance Imager (LORRI) instrument on the New Horizons mission to Pluto and the Kuiper Belt. Andy was an interdisciplinary scientist on the Galileo mission to Jupiter, a co-investigator on the Cassini mission to Saturn, a NASA co-investigator on the Japanese-led MUSES-C (Hayabusa) mission to a near-Earth

asteroid, and project scientist for the Near Earth Asteroid Rendezvous (NEAR) mission. He served as deputy chief scientist for space science in NASA's Science Mission Directorate, at NASA Headquarters, from 2007 to 2008. Andy has published extensively in the fields of astrophysics, space plasma physics, and planetary science, earning him APL's Lifetime Achievement Publication Award. His email address is andy.cheng@jhuapl.edu.



Ralph L. McNutt Jr., Space Exploration Sector, Johns Hopkins University Applied Physics Laboratory, Laurel, MD

Ralph L. McNutt Jr. is a physicist in APL's Space Exploration Sector. He received a BS in physics (summa cum laude) from Texas A&M University and a PhD in physics from the Massachusetts Institute of Technology (MIT). Ralph was a member of the Ion and Neutral Mass Spectrometer Team for NASA's Cassini mission to Saturn and is a co-investigator on NASA's Voyager, New Horizons, and Parker Solar Probe operating missions and on NASA's Europa Clipper, now under development. An author on over 220 papers, he co-chaired National Academies studies on radioisotope power systems and NASA's large strategic science missions, was the principal investigator on the study of a pragmatic interstellar probe mission for NASA's Heliophysics Division (2018–2022), chaired the nuclear power assessment study for NASA (2015), and testified to Congress on radioisotope production and lessons learned from Cassini (2017). He was chief scientist for NASA's Planetary Data System and led its 2017 roadmap study. Ralph is a member and trustee of the International Academy of Astronautics (IAA) and an associate fellow of the American Institute of Aeronautics and Astronautics (AIAA). He is a recipient of the APL Lifetime Publication Award (2020), the NASA Silver Achievement Medal (awarded to the Parker Solar Probe Team in 2019), three IAA Laurels for Team Achievement Awards (awarded to the Parker Solar Probe team in 2021, the New Horizons team in 2016, and the MESSENGER team in 2012), and 13 NASA Group Achievement Awards. Minor planet 172191 *Ralphmcnutt* is named for him. His email address is ralph.mcnutt@jhuapl.edu.